Ultragentle manipulation of delicate structures using a soft robotic gripper

Article *in* Science Robotics · August 2019

DOI: 10.1126/scirobotics.aax5425

6 authors, including:

Daniel Vogt
Harvard University
50 PUBLICATIONS **3,508** CITATIONS
SEE PROFILE

Kevin Kit Parker
Harvard University
244 PUBLICATIONS **14,981** CITATIONS
SEE PROFILE

David F Gruber
City University of New York - Bernard M. Baruch College
112 PUBLICATIONS **1,930** CITATIONS
SEE PROFILE

Robert J. Wood
Harvard University
262 PUBLICATIONS **13,259** CITATIONS
SEE PROFILE

UNDERSEA ROBOTS

Ultragentle manipulation of delicate structures using a soft robotic gripper

Nina R. Sinatra[1]*, Clark B. Teeple[1], Daniel M. Vogt[1], Kevin Kit Parker[1], David F. Gruber[2,3], Robert J. Wood[1]

Here, we present ultragentle soft robotic actuators capable of grasping delicate specimens of gelatinous marine life. Although state-of-the-art soft robotic manipulators have demonstrated gentle gripping of brittle animals (e.g., corals) and echinoderms (e.g., sea cucumbers) in the deep sea, they are unable to nondestructively grasp more fragile soft-bodied organisms, such as jellyfish. Through an exploration of design parameters and laboratory testing of individual actuators, we confirmed that our nanofiber-reinforced soft actuators apply sufficiently low contact pressure to ensure minimal harm to typical jellyfish species. We then built a gripping device using several actuators and evaluated its underwater grasping performance in the laboratory. By assessing the gripper's region of acquisition and robustness to external forces, we gained insight into the necessary precision and speed with which grasping maneuvers must be performed to achieve successful collection of samples. Last, we demonstrated successful manipulation of three live jellyfish species in an aquarium setting using a hand-held prototype gripper. Overall, our ultragentle gripper demonstrates an improvement in gentle sample collection compared with existing deep-sea sampling devices. Extensions of this technology may improve a variety of in situ characterization techniques used to study the ecological and genetic features of deep-sea organisms.

INTRODUCTION

The marine environment has long been a deep well of bioinspiration for previously unexplored materials and structures (*1*–*3*), cutting-edge medical treatments (*4*, *5*), and biomimetic manipulators and locomotors (*6*–*11*). However, it is less common for these inventions to have practical applications toward the biology and ecology of the animals from which they are inspired. Gelatinous macroplankton—including cnidarian medusae, ctenophores, and pelagic tunicates—are becoming increasingly recognized as key ecosystem consumers of energy and nutrients (*12*, *13*) and are estimated to constitute a global biomass of 38.3 Tg C (*14*). For many years, gelatinous zooplankton were overlooked by marine scientists, largely because of a lack of delicate equipment to study them, and have been referred to as "forgotten fauna" (*15*). Discoveries such as life cycle reversal (*16*) and green fluorescent protein (*17*, *18*) are two examples of findings from gelatinous zooplankton that have cross-disciplinary impacts and demonstrate the importance of learning more about these life-forms.

Despite this vast potential, collecting intact samples of gelatinous organisms to study remains extremely challenging. For example, jellyfish are composed of more than 95% water, and their mesogleal tissue has an extremely low stiffness (Young's modulus of 0.34 to 1.2 kPa) (*19*–*22*). Capturing these delicate creatures in the ocean has been a challenge for the research community because existing technologies (e.g., nets and vacuum devices) frequently damage samples during the collection process (*15*, *23*). The ideal grasping device for delicate materials in dynamic domains must incorporate a soft and flexible interface, compliant yet tough (able to absorb energy and deform plastically before fracture) appendages, and a radius of curvature compatible with the target size. This work focuses on developing a soft gripper with such properties. The target organisms for this device are three small (roughly 7 to 10 cm) jellyfish species: *Aurelia aurita*, *Catostylus mosaicus*, and *Mastigias papua*. Jellyfish present extreme challenges for delicate grasping and manipulation, and lessons learned from this exploration may be transferred to other tasks involving fragile or gelatinous objects.

Currently, state-of-the-art aquatic grippers can be classified into five categories: (i) forked metal or plastic jaws (*24*, *25*), (ii) soft hydraulic actuators (*26*, *27*), (iii) jamming grippers (*28*), (iv) suction samplers (*29*), and (v) noncontact containers that close around a swimming animal (*30*). Metal or plastic grippers are the most widespread marine sampling method due to their use in oil and natural gas industries, but their rigid surfaces can snag or compress gelatinous animals, and a fixed radius of curvature is unable to conform controllably to the shape of amorphous or soft-bodied animals (*31*). Foam-coated hydraulic actuators have substantially improved nondestructive sampling of delicate benthic and midwater animals (e.g., coral and sea stars) by decreasing grip force while increasing pressure distribution (*26*). However, the contact pressure exerted by foam-covered actuators (1 to 10 kPa) is too high to grasp gelatinous animals without causing harm (fig. S4). Although particle jamming grippers are capable of lifting sedentary objects, their operating mechanism is not well suited for grasping floating organisms (*28*, *32*). Suction samplers use a pump to draw an untethered animal through an inlet tube and into a storage container; however, delicate organisms can be damaged as they move through the tubing (*30*, *33*).

Last, noncontact tools such as the detritus sampler ("D-Sampler") or the RAD (rotary-actuated dodecahedron) sampler are open containers that are positioned near floating specimens and then closed around the organism. Use of the D-Sampler with remotely operated vehicles (ROVs) is challenging because the container is typically positioned by moving the entire vehicle (*30*, *34*). Although the RAD sampler (*30*) has successfully captured centimeter-scale squid and octopi, misalignment of the container (an origami-inspired structure that folds to form a sealed dodecahedron) as it closes can trap and cleave

[1]John A. Paulson School of Engineering and Applied Sciences and the Wyss Institute for Biologically Inspired Engineering, Harvard University, 29 Oxford Street, Cambridge, MA 02138, USA. [2]Department of Natural Sciences, Baruch College, City University of New York, 55 Lexington Ave., New York, NY 10010, USA. [3]PhD Program in Biology, Graduate Center, City University of New York, 365 5th Ave., New York, NY 10016, USA. *Corresponding author. Email: sinatra.nina@gmail.com

the tentacles of fragile specimens. A flexible, compliant gripper is needed to bridge this capability gap, thereby achieving nondestructive grasping of gelatinous marine organisms. In this study, we report a multi-scale approach for gentle grasping using nanofiber-reinforced soft actuators.

Previously, we developed flexible and robust microscale soft actuators composed of an elastomer matrix reinforced with polymer nanofibers (*35*). Nanofibers were selected as the strain-limiting layer because of their ease of processing and high specific strength; the actuators underwent large deformations without requiring stiffer reinforcing materials, such as carbon or glass fibers. Furthermore, the nanofabric's high surface area facilitated bonding with elastomeric materials during the fabrication processes and demonstrated no delamination from the matrix after tensile testing of the actuator to failure. Unlike our previous nanofiber-reinforced polydimethylsiloxane microrobots (whose matrix has a Shore hardness of 43), the mesoscale actuators presented here incorporate a lower durometer silicone matrix (Shore 20A), which is better suited for interacting with fragile structures. Here, we leverage the flexibility and durability of these materials to engineer mesoscale soft hydraulic actuators.

Our grasping device is composed of six composite actuator "fingers" connected to a three-dimensional (3D)–printed "palm" produced using a PolyJet-based printer (Objet Connex500, Stratasys). Each actuator contains an elastic yet tough silicone matrix and a strain-limiting layer of flexible polymer nanofibers. The gripper is lightweight (123 g) and can be actuated using very low hydraulic pressure (1 to 6 psi, or 6.9 to 41.4 kPa, with respect to ambient).

Upon pressurization, a channel within each actuator inflates, and the appendage bends in the direction of the stiffer fiber-reinforced layer. Inflation of several actuators spaced around a marine organism enables the animal to be gently cradled by the soft silicone digits. The actuators overlap and contact one another, forming a soft network that restricts the position of the target but does not fully immobilize it (*36*); this caging grasp reduces the need to precisely control individual finger placement and instead relies on collective inflation of all actuators. The low contact pressure exerted by each actuator (0.0455 ± 0.007 kPa) also facilitates nondestructive interaction. To better understand the device's performance space, we empirically identified the region of acquisition using a synthetic target and quantified the resistance to forces on the object during a grasp. The soft gripper can be adapted both to deep-sea exploration using an ROV (Fig. 1A) and to portable specimen collection in the shallower waters of the photic zone. Last, we demonstrate the use of the portable device setup to successfully grasp three jellyfish species (Fig. 1, B to D).

RESULTS

Design criteria for ultragentle gripper

The objective for this device is to perform nondestructive grasping of gelatinous marine organisms in the marine environment. We identified several performance requirements to ensure successful function. First, because the gripper will be fully submerged in the ocean during operation, it must be composed of materials that are resistant to corrosion in salt water. To fulfill this aim, we selected a silicone matrix, nylon and polyurethane reinforcing fiber, PolyJet palm chassis, and stainless steel fasteners, each of which is undamaged by seawater immersion during the operational life cycle of this device (several weeks) (*37*–*41*). Second, the materials must withstand use at typical ocean temperatures, which reach a minimum of 0° to 3°C in the deep sea (several thousand meters) and a surface average of 17°C. The operational range of all the materials listed above is within this window; for example, silicone rubbers are highly resistant to low temperatures and have an embrittlement temperature between −20° and −30°C (*42*). Because of the design of the hydraulic pump used to inflate the soft fingers (*26*), pressure within the actuators is equalized to that of the surrounding waters and is therefore not a barrier to operation.

The following design criteria relate to the organisms that the gripper will be required to interact with. The actuator length must be determined by the average size of the intended object or species. Although gelatinous animals exist in a variety of shapes and sizes, we selected three of the most widely studied jellyfish species to serve as models: *A. aurita*, *C. mosaicus*, and *M. papua*. The average bell diameter for these species is 7 to 10 cm (*43*, *44*). To fully enclose the body of the selected jellyfish, the total length for our actuators must exceed this amount and was set at 15 cm. However, actuator size may be easily scaled to accommodate larger or smaller organisms. Larger actuators may require thicker nanofiber sheets near the distal tip to maintain uniform curvature throughout the length of the actuator. During extended operation, a small amount of air can become trapped in this area of the internal channel. The silicone membrane will deform more around the enclosed air than around water, leading to higher local curvature at the distal end (i.e., the "finger tip" will bend more than the rest of the actuator). Last, to execute a nondestructive grasp, the contact pressure exerted by each actuator should be below 1 kPa, the current state of the art for soft marine grippers (*26*). We have evaluated the pressure exerted by our composite actuators in a subsequent section.

Robotic palm design

The soft robotic gripper includes six modular actuators attached to a custom-designed, 3D-printed hub (Fig. 2B) composed of a transparent photopolymer (RGD720, Stratasys). The appendages are individually attached to the central palm and may be removed or exchanged in the case of actuator failure or to experiment with different digit configurations. The set of actuators are pressurized hydraulically (Fig. 2C) using a single channel at the back of the hub, which can be attached to a fluid source using quick-disconnect fittings. In the present configuration, the actuators were evenly spaced, with two on either side of a 78-mm rectangular palm and one on either end of the opposite 45-mm edge. This layout was chosen because adhesion and friction between actuators on either side of the hub resulted in a strong caging grasp (fig. S7). The actuators placed at the top and bottom of the palm prevent a target object from being released at either end and contribute to a caging grasp by overlapping the center actuators. Actuator position can be rapidly adjusted by modifying the 3D-printed hub design. Additive manufacturing supports iterative development of soft grippers with varying numbers and positions of actuators (e.g., a hexagonal hub with six actuators or a circular palm with 10 digits). This flexibility can enable further customization to support organisms with specific shapes and symmetries (*27*).

Actuator design

Understanding the impact of geometric and process variables during actuator fabrication is crucial to regulating input pressure range and reducing manufacturing defects. Three key design parameters can be tuned toward achieving these goals: interior channel height, thickness of the inflating membrane, and thickness of the adhesive layer during the cobonding process (illustrated in Fig. 3A). Each of

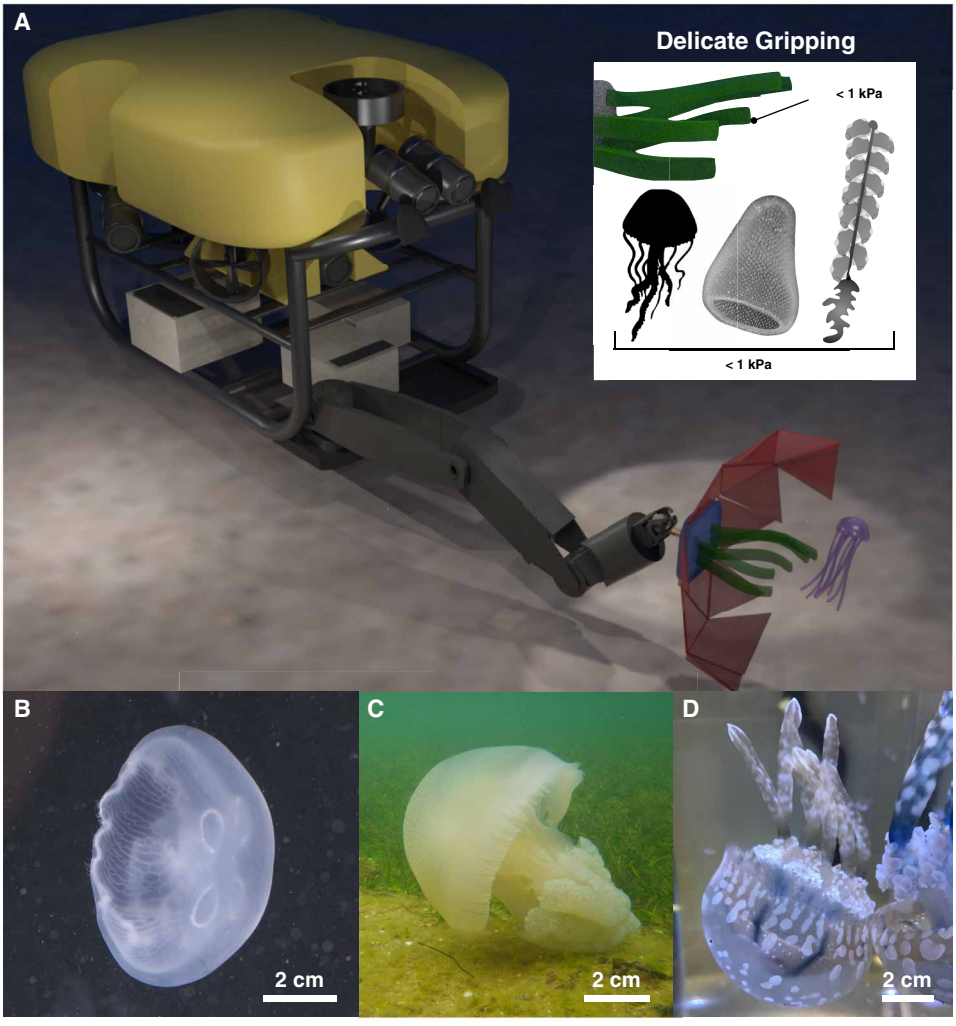

Fig. 1. Soft robotic actuators are a promising approach to grasping fragile marine organisms. (**A**) Illustration demonstrating the envisioned application of soft robotic actuators (green) attached to an ROV. These actuators were designed for ultragentle manipulation of delicate tissues, such as jellyfish and other gelatinous marine species. The target species for our soft gripper are (**B**) *A. aurita*, (**C**) *C. mosaicus* (photo credit: Peter Campbell; www.greenlivingpedia.org/Image:Blue_Blubber_Jellyfish_IMGP2102.JPG), and (**D**) *M. papua*.

these parameters was compared against two success metrics: the actuator failure pressure and the number of defects observed during manufacturing. The defects formed during the process of cobonding the concave portion of the interior channel (already cured) to a thin cast film of uncured silicone (which forms the upper membrane enclosing the channel). These irregularities were small cylindrical pillars spanning the top and bottom of the channel, which formed after the cured part was placed onto the film. We hypothesize that these pillars formed as a result of surface tension drawing the uncured liquid toward the center of the channel, forming a Gaussian-shaped mound that eventually contacts the opposite side of the channel. For each batch of actuators, the total number of actuators with "pillar" defects and the burst pressure of each actuator under pneumatic actuation were measured. We assumed that the relative difference between the burst pressure of actuators with and without nanofiber reinforcement would be similar when actuated hydraulically and pneumatically.

To begin our assessment of the impact of the three design parameters on actuator burst pressure and defect percentage, we varied the interior channel height. The channel height can be tuned by modifying the 3D-printed mold that was used to form the thicker portion of each actuator. Three molds were printed, with channel heights of 0.3, 0.4, and 0.5 mm. For fixed membrane (0.25 mm) and adhesion layer (0.05 mm) thicknesses, a 0.5-mm channel displayed the highest failure pressure (Fig. 3B). Thus, we selected this height for all subsequent actuators. Next, channel membrane thickness was varied from 0.25 to 0.35 mm in 0.5-mm increments, using a constant channel height (0.5 mm) and adhesion layer thickness (0.05 mm). We observed an increase in burst pressure with membrane thickness; the 0.35-mm membrane displayed significantly higher burst pressure than the two thinner options (Fig. 3C). This is a logical result, because imposing a thicker barrier against applied pressure will require a higher pressure to induce a rupture. Although the failure pressure of actuators with a 0.35-mm membrane was acceptable on the basis of current operational requirements for ROV-mounted robots, a wider range of membrane thicknesses may be explored to accommodate higher pressure requirements.

Last, adhesion layer thickness was varied (set to either 0.03 or 0.05 mm), and burst pressure and defect percentage were measured for actuators with a constant channel height of 0.5 mm and a 0.35-mm membrane. The 0.03-mm adhesive layer yielded a significantly higher percentage of pristine (lacking fabrication defects) actuators for a slightly (albeit not statistically significantly) higher burst pressure, as compared with the thicker adhesive layer (Fig. 3D). Scanning electron micrographs of actuator cross sections revealed that the thinner adhesive layer yielded a uniform membrane thickness across the width of the channel (Fig. 3E). In contrast, capillary action resulted in a nonuniform membrane when a 0.05-mm adhesive layer was used. Thus, we selected the following parameters for all subsequent soft actuators: 0.5-mm internal channel height, 0.35-mm channel membrane thickness, and 0.03-mm adhesion layer thickness.

We also noted that the failure pressure of pneumatically pressurized nanofiber-reinforced actuators was significantly higher than that of silicone-only actuators (both fabricated with the previously listed parameters; fig. S6). In addition to decreasing the overall actuator curvature, incorporating a fibrous reinforcement layer increased the toughness and stiffness of the device while maintaining the extensibility of an elastomer-only layup (*35*). Although tuning the nanofiber elastic modulus can affect the overall curvature of the soft actuator, the impact of other design parameters (e.g., fiber layer thickness and orientation)

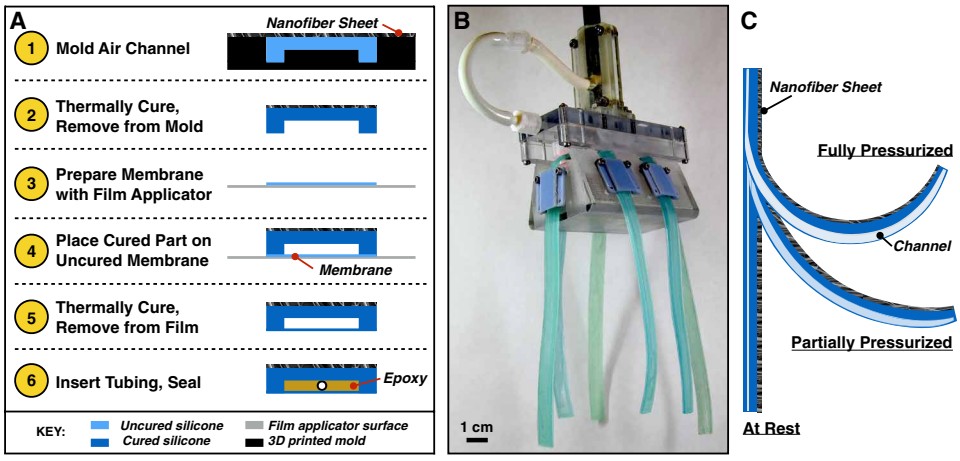

Fig. 2. Fabricating nanofiber-reinforced soft robotic actuators. (**A**) Actuators were manufactured using molding and cobonding (cross-sectional view shown). (**B**) Six soft actuators connected to a 3D-printed hub. (**C**) As an actuator is pressurized, the internal channel inflates and the device bends toward the strain-limiting nanofiber layer.

may be investigated in future studies using analytical models developed in a previous analysis (*35*).

Quantifying contact pressure exerted by individual actuators

One benefit of using soft robotic actuators for gentle manipulation is that the contact pressure exerted by each appendage can be lower than that of traditional rigid (e.g., metal) end effectors. To assess the contact pressure of our device, we pressurized individual actuators while in contact with a stationary load cell. At their typical operating pressure of 6 psi (41.4 kPa), nanofiber-reinforced soft actuators exerted an average contact pressure of 0.0455 ± 0.007 kPa (mean ± SEM), which is well below the target of <1 kPa. A representative plot of one actuator being hydraulically pressurized and depressurized over four cycles in shown in fig. S2B. These results confirm that our soft actuators exert a low, safe pressure on target objects and organisms.

Evaluation of underwater grasping performance

The performance of our ultrasoft robotic gripper was empirically evaluated on the basis of two standard grasp quality metrics: the size of the region of acquisition (*45*) and the robustness to external forces on the object (*46*, *47*). Both metrics can be used to inform potential end users (ROV pilots) about how to best use the capabilities of this gripper when mounted on a teleoperated ROV.

Gripper's region of acquisition

The region of acquisition of a grasping device is defined as the set of all positions (relative to a target object) that the gripper can be placed to reliably grasp the target (*45*). For this ultragentle hand, we first made a rough map of a planar slice of this 3D region and then performed higher-fidelity testing along key axes. On the basis of the estimated region of acquisition, we can gain insight into the precision required to reliably grasp objects when the hand is mounted to the arm of an ROV.

A slice of the region of acquisition (located about 5 mm behind the target) was estimated empirically by performing a series of grasps on a surrogate target: a silicone model jellyfish. This target was selected on the basis of its morphological similarity to a living jellyfish and because its bell diameter is on the order of that of the species of interest for this study. To capture the entire region, we performed a sweep over a grid of centering positions ($n = 2$ grasps per position) 160 mm wide and 120 mm high, with a step size of 10 mm in both directions (Fig. 4A).

To quantitatively asses gripper performance at each centering position, we determined the grasp success rate by observing the number of successful grasps. A grasp was considered successful if the target was moved to its final position and remained there until it was released. If the target was released early or was not grasped, the attempt was considered a failure. The grasp success rate at a given hand position was then calculated as the number of successful grasps normalized by the total number of attempts. Further refinement of the acquisition region was obtained by performing higher-repetition sweeps ($n = 5$) along key axes associated with the 3D volume of the region. The axes tested include the vertical axis (z) through the center of the region, one side of the horizontal axis (y) through the center, and the axis directly behind the center of the object (x). The resulting grasp success rates are shown in Fig. 4 (C to E).

By examining the shape of the region where successful grasps occur, we can quantify the positioning and precision necessary for reliable grasping. The general shape of the region is a diamond (roughly symmetric about the vertical axis), as shown in Fig. 4A. This shape is logical considering the placement of actuators around the rectangular palm. In addition, unsurprisingly, the center of the main region is located 10 mm below the center of the object, which can be explained by slight buoyancy of the soft actuators due to trapped air. The characteristic dimension of the region of acquisition can be found by the radius of the largest circle that can be completely contained within the boundaries of the main region (conservative metric). For our gripper, this radius is about 42 mm. Last, we observed that grasps toward the center of the region consistently demonstrated caging grasps, whereas locations along the edge of the region displayed a wider variety of grasps (hooking under the bell or wrapping around tentacles).

Gripper's robustness to external forces

The robustness to external forces and torques on an object during a grasp is typically defined as the maximum force the gripper can resist (or conversely, the minimum force required to pull an object out of the grasp), minimized over all force application angles (*46*). This measure of robustness can be used to understand how to maneuver an ROV arm to transport delicate samples to a storage container. To quantify how the angle of applied force affects the robustness, we executed grasps on the same synthetic jellyfish target. After grasping, force was applied at a prescribed angle until the target slipped out of the gripper. The process was repeated five times for angles ranging from 0° (perpendicular to the palm) to 90° (parallel to the palm) in increments of 15° (Fig. 5A). We assumed that the relationship is symmetric about the x-z plane based on the symmetry of actuator placement.

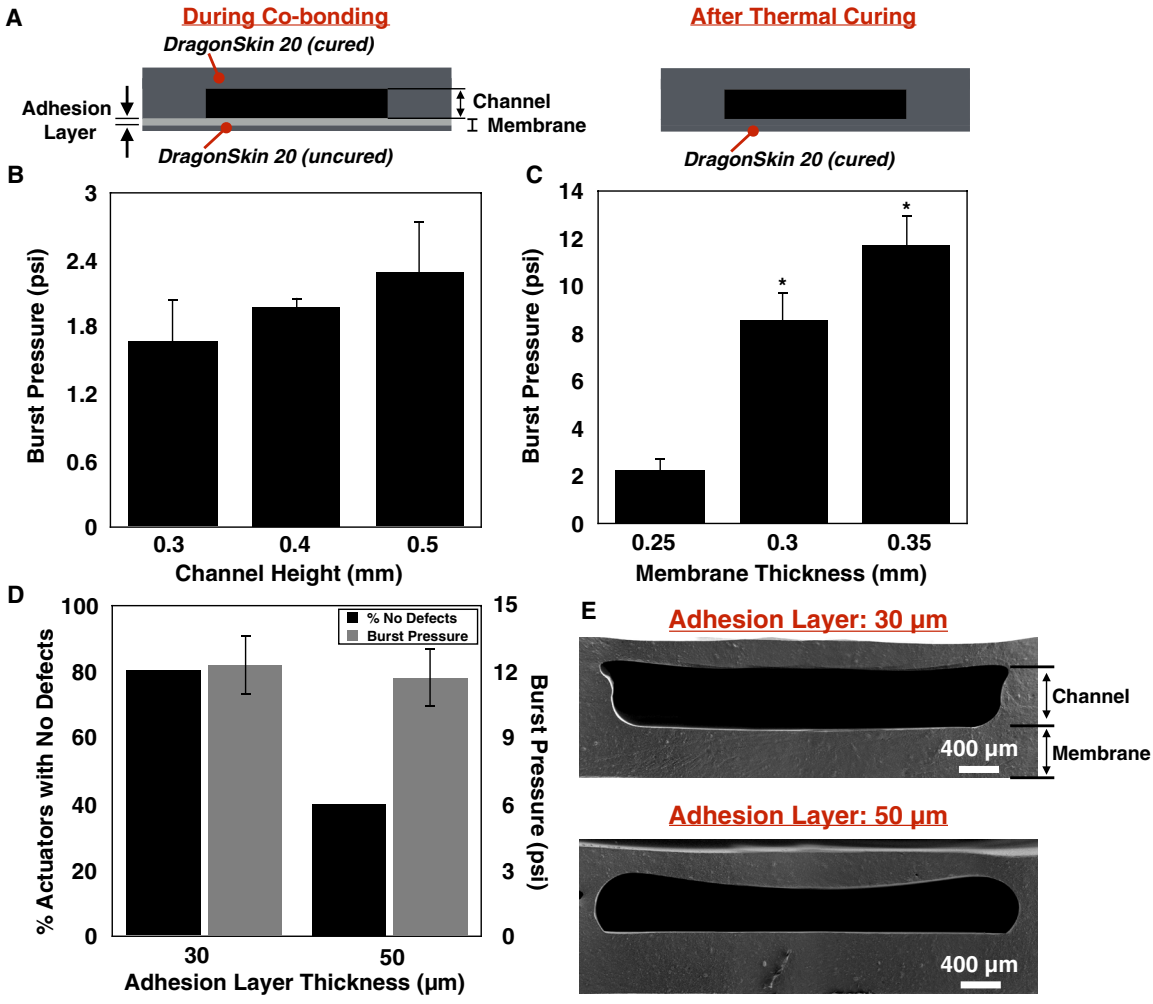

Fig. 3. We evaluated the effect of actuator geometry on burst pressure and percentage of defects. (**A**) Cobonding cured actuator section to uncured silicone layer. (**B**) Actuator burst pressure as a function of internal channel height, with a constant membrane thickness of 0.25 mm (mean ± SD, $n = 4$ actuators). (**C**) Burst pressure as a function of membrane thickness (mean ± SD, $n = 4$ actuators). *$P < 0.05$. (**D**) % pristine actuators and burst pressure as a function of adhesion layer thickness (mean ± SD, $n = 5$ actuators). (**E**) Scanning electron micrographs of actuators with 30- and 50-μm adhesion layers (cross section).

Our results indicate that the gripper's ability to withstand external forces improved as the force application angle increased from 0° to 60°, whereas the grasp success rate decreased as a function of the angle (Fig. 5B). The worst-case scenario for our gripper involves pulling the target object straight back at an angle of 0° with an average maximum pull force of 0.20 ± 0.04 N. As the angle increased, the mean and variance increased until 60°, where the maximal pull force increased to 0.77 ± 0.40 N. In addition, the initial grasp success rate was 100% for angles 30° and below but decreased as a function of the angle until 75°, where grasping was no longer possible.

To understand the trend in the maximum force as a function of the applied angle, we can draw one possible insight from treating the ultrasoft actuators as tensile members with interactions between fingers treated as "weak points," as discussed in the Supplementary Materials. On the basis of this simplification, we find that tensile forces are not shared equally between all fingers, and shear forces between two fingers have a critical breaking point. This critical shear force causes the fingers to release the object at a certain applied force, which increases as a function of the applied angle (fig. S7).

Evaluating grasp quality as a function of gripper motion

During a typical deep-sea biological sampling operation, the act of moving an animal after grasping it produces forces on the animal due to fluid drag. To understand how this effect manifests during a grasping operation, we performed grasps on the same artificial jellyfish with the gripper positioned on center, but with varying retraction speeds from 0.0080 to 0.200 m s^{-1}. At lower speeds (0.008 to 0.050 m s^{-1}), the object remained within 10 mm of the initial position (with respect to the gripper) for the entire duration of the retraction motion. However, as speed increased beyond 0.050 m s^{-1}, a large increase in extraneous motion due to fluid drag during retraction was observed. Thus, the speed at which the target is pulled could potentially have a substantial impact on the stability of the grasp.

To further understand the maximum speed needed for an object to be pulled from the gripper due to fluid drag alone, we calculated the drag in water on our target jellyfish (approximated as a hemisphere), as discussed in the Supplementary Materials (fig. S5). On the basis of the average grip force measured at a 0° pull angle (0.2 N), we

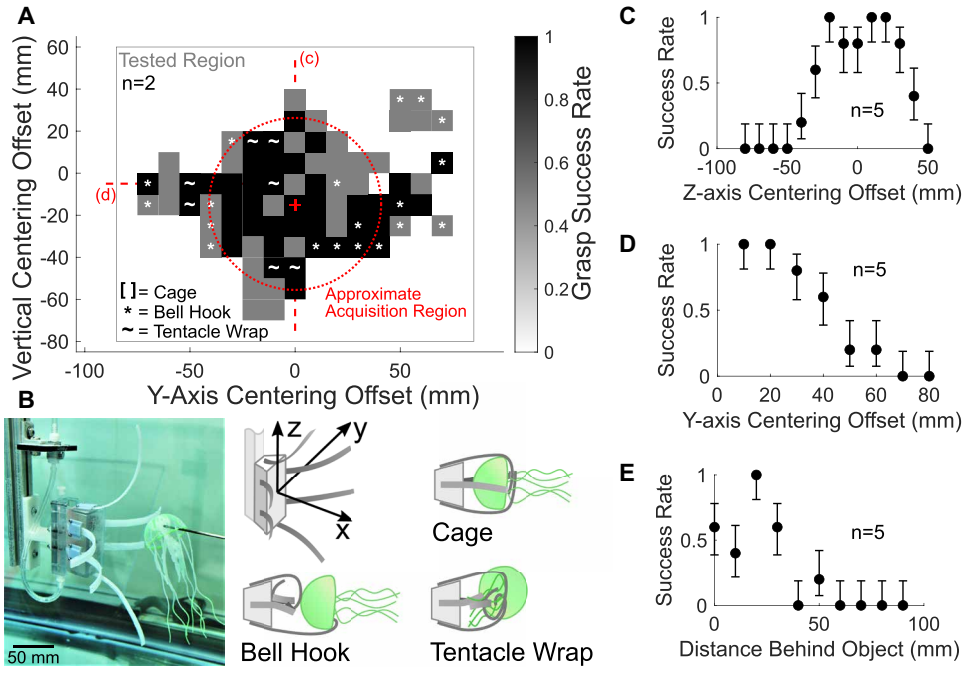

Fig. 4. We mapped the region of acquisition of our soft gripper using our water tank testing setup. (**A**) A coarse estimate ($n = 2$) of the region indicates a roughly diamond shape, and (**B**) various grasp types were observed, including cage grasps, bell hooks, and tentacle wraps. A higher-fidelity investigation along (**C**) the vertical axis, (**D**) the *y* axis, and (**E**) the *x* axis behind the target was performed with $n = 5$ grasps for each condition. Error bars in (C) to (E) represent the 95% Agresti-Coull confidence interval.

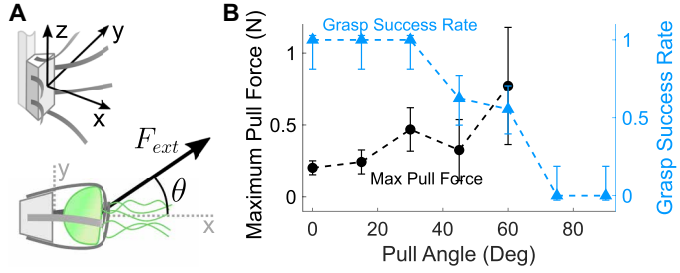

Fig. 5. We evaluated the robustness of our gripper to external forces on a target object. (**A**) The target was grasped by our soft actuators and pulled out at an angle. (**B**) The maximal external force before failure increased as a function of the angle applied while the grasp success rate decreased. Error bars represent the SD for pull force measurements, and the 95% Agresti-Coull confidence interval for grasp success rate estimates. $n = 5$ successful grasps per condition, except 75° and 90°, where $n = 5$ attempts were made.

found that a velocity above 0.7 m s^{-1} would be required to dislodge a jellyfish from the soft gripper. Because all of our grasp quality testing was performed using a 0.080 m s^{-1} retraction speed (roughly one-ninth the estimated maximum speed before failure from fluid drag), we assume that all of our results represent quasistatic grasping. In addition, these estimates may help inform operators on how fast to maneuver ROV arms while attempting to sample these delicate animals.

Preliminary field testing of soft robotic gripper

Although these soft actuators are compatible with the manifold system (which regulates actuator pressurization) of existing ROVs, we aimed to test the viability of our robotic gripper outside a laboratory setting. To achieve this goal, we developed a portable, hand-held device to operate the soft gripper (Fig. 6A). Having characterized the performance of the soft actuators in controlled laboratory tests, we sought to demonstrate gentle grasping using live jellyfish. Adult *A. aurita* (Fig. 6B), *C. mosaicus* (Fig. 6C), and *M. papua* (Fig. 6D) housed at the New England Aquarium (Boston, MA) served as the target organisms (Animal Care and Use Committee protocol no. 2018-09). We demonstrated that once a jellyfish was enclosed securely by the actuators, it was unable to break the grasp. In all cases, the jellyfish displayed no adverse effects or changes in behavior after the interaction.

Given that our soft actuators overlap cooperatively in a caging grasp during pressurization, we asked whether the number of actuators on a palm could be varied. Rectangular palms containing four and six appendages were tested for their efficacy in grasping and restraining jellyfish. The four-actuator palm measured 60 mm (length) by 50 mm (width), with two digits on each side of the longer edges. The six-actuator hub measured 78 mm by 45 mm and featured an additional actuator on the top and bottom edges. Both setups were capable of grasping the gelatinous animals, but the six-actuator device displayed a more secure grip. In several (15 to 25%) trials using the four-actuator palm, the appendages began inflating around a jellyfish, but the animal swam toward the top or bottom edges and evaded capture. This observation led to design revisions featuring an additional set of actuators that contributed to a more effective caging grasp. The addition of an extra actuator at both ends improved grasp quality by gently restraining the jellyfish within the inflated actuator network.

During both laboratory tank testing and the pilot field study, each set of actuators was pressurized and depressurized about 100 times before a failure was observed. The failure was a rupture in the membrane enclosing the inflating channel of an individual actuator. During the lifetime of an actuator, the elastic membrane can become distended because of rapid pressurization or applying an input pressure above 8 psi (55 kPa). Eventually, a ~1-cm tear may occur in the distorted membrane, at which time the actuator will be inoperable. The modular design of the soft gripper hub enabled the faulty part to be removed and a new actuator to be inserted in its place.

DISCUSSION

Here, we have demonstrated an approach to design, manufacture, and test nanofiber-reinforced soft robotic actuators for ultragentle manipulation of delicate marine organisms. Specifically, we discussed the geometric optimization of individual actuators to increase durability and batch throughput and the design of a modular hub to unite a set of actuators into a gripping device. Moreover, we described two

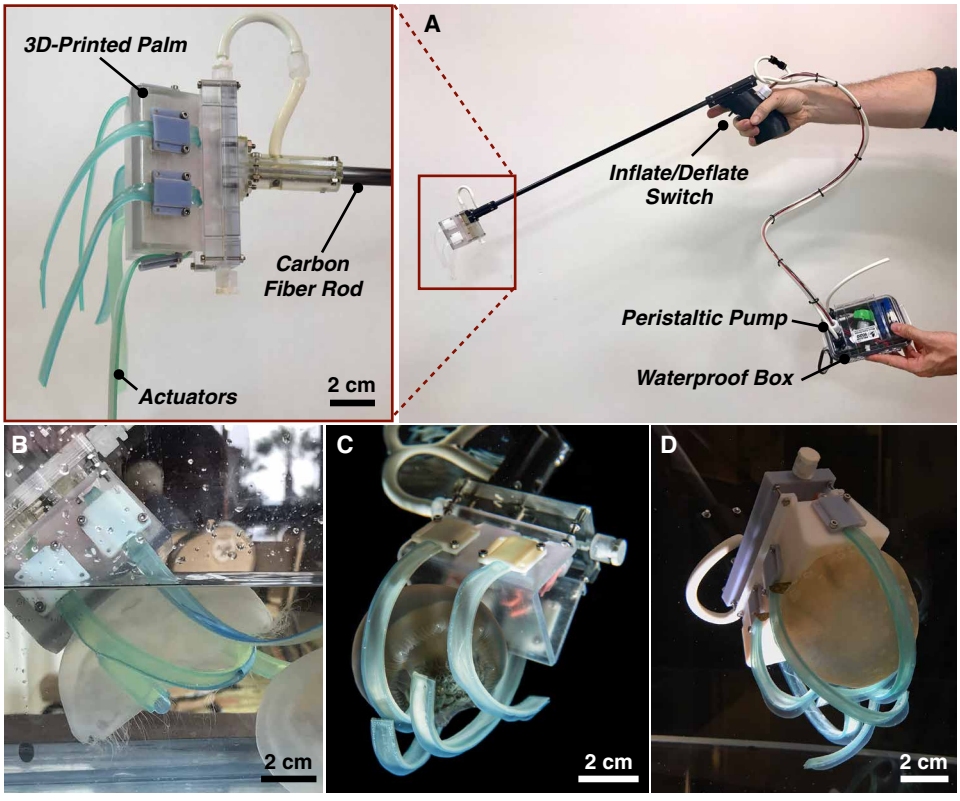

Fig. 6. A handheld grasping device was developed to test our soft actuators outside the laboratory. (**A**) Design of soft robotic gripping device, shown with a four-actuator hub. Inset: Different hubs, including this six-actuator palm, can be attached modularly. Soft fiber-reinforced actuators grasping (**B**) *A. aurita*, (**C**) *C. mosaicus*, and (**D**) *M. papua*. (C and D) Photos courtesy of Anand Varma.

important grasp quality metrics: the region of acquisition of the gripper in a rectangular configuration and the robustness of its grasp to applied force. Next, we incorporated the device into a portable tool that can be used to interact with biological specimens in a laboratory or in shallow marine environments. Last, we demonstrated the use of this hand-held soft gripper to successfully perform gentle grasping of three canonical jellyfish species.

Generalizing laboratory grasping performance

The region of acquisition measured for our gripper provides insight into the precision needed to reliably grasp objects. On the basis of the circular region characterized with a 5-mm distance behind the object, we can estimate that a lateral centering offset within 42 mm of the target will result in at least a 50% chance of a successful grasp. In addition, the gripper has better performance when translated directly along the y or z axes (radii of 50 and 65 mm, respectively). Moreover, the gripper was able to grasp objects up to 50 mm behind the target (x axis), albeit with high variability in grasp success (Fig. 4E).

Although we would expect consistently high grasp success near 0-mm centering offsets, the observed nonperfect performance in Fig. 4 (C and E) likely stems from natural variation in the grasping process. Together, this information can be used to inform ROV operators of positioning requirements to most effectively use this gripper.

In addition, passive adaptation of fingers enables the gripper to robustly achieve grasps in a larger region. Most of the grasps within the main region were cage grasps, indicating that caging is a primary grasping mode for this gripper. The success of caging grasps generalizes to real organisms, as shown in our preliminary field testing. Conversely, grasps along the edges and outside the main region included higher occurrences of marginally stable grasps. These grasps use the passive compliance of soft actuators to hook around the bell or curl around tentacles. Although less reliable, these grasps represent a family of edge cases where the fingers passively adapt to grasp the target in positions where caging would likely fail. However, the success of these marginal grasps may not generalize to the actual organisms because they rely on the strength of the bell and tentacles.

Although the laboratory and pilot studies presented here focused on grasping either a stationary target or a live jellyfish in an enclosed space, these results show promise toward ROV-mounted actuator operation in the ocean. Wild jellyfish display a variety of movements and swimming speeds, from the sedentary *Cassiopea* to the complex swimming behaviors of *Cubozoa* (box jellyfish) (*48*, *49*). Most jellyfish have a slight negative buoyancy and must swim to survive and feed in the water column. For example, *C. mosaicus* swims at a rate of under 60 cm min^{-1} (*50*) both against and along the background current. The average swim speed of *A. aurita* depends on the direction of motion and ranges from 176 to 233 cm min^{-1} (*51*).

Despite diversity in movement characteristics, an ROV-mounted high-torque underwater pump and pressure regulator will make it possible to grasp gelatinous organisms. When operating soft actuators using an ROV, pressure regulation would ensure that the actuators will not be overpressurized (excess pressure will reduce operating life) and that sufficient flow will enable them to close in a sufficient amount of time. We expect that the differences between positioning the gripper on an ROV and using the portable device will depend on the type of ROV robot arm that is used and the skill of the ROV pilots. We see promise in the work of Teoh *et al.* (*30*), showing that adept pilots could encase jellyfish at depth with an ROV-mounted manipulator.

Last, our gripper's robustness to external forces is large enough to prevent organisms from being released after they are captured. Even the worst-case pull force (0.20 ± 0.04 N at 0° pulling angle) is two orders of magnitude greater than the theoretical thrust force of 0.002 to 0.004 N generated by *A. aurita* (derived in the Supplementary Materials). Furthermore, when the gripper is en route to a sample collection container, the worst-case estimate for the maximum speed before drag from the water causes the fingers to release (0.7 m s^{-1}) is still very reasonable for typical ROV operation.

These results represent an unprecedented capability for delicate manipulation of fragile tissue samples. Although other fiber-reinforced

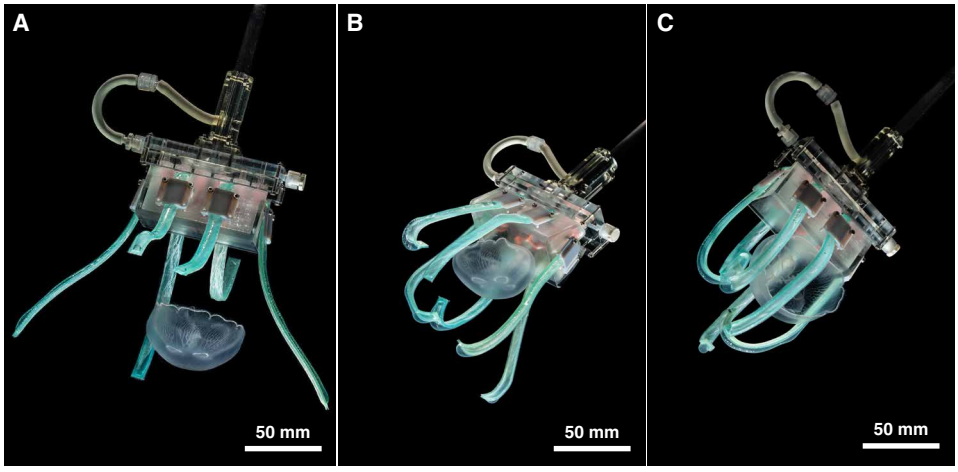

Fig. 7. Gentle grasping of *A. aurita*. (**A**) Actuators approach the jellyfish, un-inflated. (**B**) Actuators begin to hydraulically pressurize. (**C**) Actuator pressurization continues until the jellyfish is gently and securely grasped. Photos courtesy of Anand Varma.

soft actuators have been developed to grasp delicate marine species (e.g., corals and sea cucumbers), factors such as higher contact pressure and grasp style (e.g., power grasp versus caging grasp) limited their ability to safely interact with gelatinous soft-bodied animals. Our soft robotic actuators offer the opportunity for nondestructive interaction with and investigation of extremely delicate marine organisms whose study had previously been limited by existing collection paradigms.

In the future, we believe that extensions of this work will enable further advances in delicate grasping for the study of ocean-dwelling organisms and beyond. For example, in situ characterization of physiological and genomic properties of animals could be achieved through integration of sensors into these ultragentle actuators (*52*, *53*) and using deep neural networks to automate tasks such as species identification (*54*). When combined with other existing sampling mechanisms, such as deep sequencing on a small sample from a single organism (*55*), in situ measurements and data collection may enable biologists to better understand and conserve deep-sea biodiversity.

MATERIALS AND METHODS

Fabrication of nanofiber-reinforced soft actuators

The objective of this study is to design and fabricate a gentle gripper capable of nondestructive sampling of soft-bodied marine organisms. To accomplish this goal, we developed a soft composite actuator composed of a silicone rubber matrix and a flexible, yet tough, nanofiber reinforcement layer. It is important to consider the mechanical properties of silicone with respect to those of the target organisms and in the context of the robot's operational environment. Although the elastic modulus of Dragon Skin 20 (measured as 0.37 MPa) is an order of magnitude larger than that of jellyfish mesogleal tissue (0.34 to 1.2 kPa) (*19*–*22*), the durometer of this silicone (Shore 20A) provides durability and failure resistance under high applied pressures (*56*).

Composite soft actuators were produced as per the approach outlined in Fig. 2A. First, the lower portion of the actuator was fabricated. Uncured silicone rubber (Dragon Skin 20, Smooth-On Inc., Easton, PA) was poured into a custom-designed 3D-printed mold, and the assembly was degassed in a vacuum chamber for 10 min. Next, a nanofiber sheet was placed on the mold, enabling the uncured silicone to permeate the fabric. Nanofabric sheets [3 weight (wt)/volume % nylon-6 (Nylon 6, Sigma-Aldrich, St. Louis, MO)/3 wt/volume % polyurethane (McMaster Carr, Princeton, NJ)] were manufactured using rotary jet spinning, according to protocols discussed in previous studies (*35*, *57*, *58*).

For all tank and field studies, pristine fiber sheets were embedded into soft actuators at a fiber orientation angle of 0° (parallel to the longitudinal axis of the actuator). The component was thermally cured at 75°C for 15 min and removed from the mold. Then, the upper portion of the actuator (a thin membrane enclosing the internal channel) was fabricated. A layer of uncured silicone was generated using a film applicator, and the cured component was placed onto this film. By cobonding the upper and lower parts together, we formed the internal channel that was pressurized to actuate each device.

Last, the components were thermally cured (75°C, 15 min), tubing was inserted into the channel opening, and the area around the tubing was sealed with epoxy (Sil-Poxy, Smooth-On Inc., Easton, PA). For selected field tests, several drops of Smooth-On Silc Pig silicone dye was added to the uncured Dragon Skin 20 during actuator production; the purpose of this pigment was to improve the visual contrast between the soft actuators and surrounding water. The minute volume of dye added to the mixture did not affect thermal curing of the silicone rubber.

Measuring actuator contact pressure

To gauge the contact pressure of our device, we measured the blocked force exerted by the tip of each actuator (the part likely to make contact with a target object) using a stationary 10-N load cell (2530-10N, Instron, Norwood, MA) connected to a plate. Blocked force represents the maximum force that can be generated by each actuator. To minimize gravity effects, we mounted actuators vertically with the distal tip pointing downward (fig. S2A). The distal end was secured in a 3D-printed fixture, which was attached to the plate. Each actuator was then pressurized hydraulically, and the blocked force exerted by the actuator tip on the fixture was recorded using Instron Bluehill 3 Testing Software (Instron 5544A, Norwood, MA). Last, the contact pressure exerted by an actuator was calculated using the area of the fixture and the measured force.

Laboratory evaluation of gripper performance

We evaluated the performance of our ultragentle robotic gripper using a custom-built testing platform designed for repeated testing of grasping operations underwater. The underwater environment was a glass tank of about 60 cm wide by 180 cm long by 75 cm tall filled with tap water. To position the gripper in 3D space, we mounted a custom three-axis gantry above the tank, with an arm extending down into the tank. The gripper was mounted to this arm and could

be positioned within a region of 100 cm by 40 cm by 50 cm inside the tank. The soft actuators were driven hydraulically with a custom control system that supplied precise input pressure. Robot Operating System (*59*) was used to coordinate motion, pressure control, and a camera for documentation purposes.

The target object (a synthetic jellyfish) was positioned away from the walls of the tank using a thin tube connected to a positioning wall. The soft silicone rubber target was similar in shape and compliance to its biological counterpart. To ensure precise repositioning of the target object before each grasp attempt, we mounted the object on a Kevlar tether that was routed out of the tank via a low-friction pulley system. When force was applied to the tether, the target was moved back to within 2 mm of its initial position and within ±10° of its initial orientation about the *y* and *z* axes. Because of radial symmetry, the orientation of the target was not controlled about the *x* axis.

When mapping the region of acquisition, each grasping operation consisted of an approach, grasp, retract, and release cycle, as shown in fig. S1. For each centering position, the palm of the gripper was initially located 350 mm behind the target. The gripper then approached the target, and a grasp was attempted by inflating the actuators to 6.0 psi. Last, the gripper attempted to pull the target to a new position (200 mm behind the initial centering position) and released it (by depressurizing the actuators) in preparation for the next test. Movie S1 shows an example of a typical grasping test. All tests were performed at low speeds (0.080 m s^{-1}) to ensure minimal fluid drag with the target and fingers.

To quantify the maximum external force as a function of the applied angle, we executed grasps on the same synthetic jellyfish target. Then with zero centering offset, the palm was retracted and then paused while force was applied on the object through the Kevlar tether at a prescribed angle. Force was applied by adding constant increments of mass to a plastic container at the end of the tether (connected via low-friction pulley system to the target object) until the target slipped out of the gripper. The process was repeated five times for angles ranging from 0° (perpendicular to the palm) to 90° (parallel to the palm) in increments of 15° (Fig. 5A). We assumed that the relationship is symmetric about the *x*-*z* plane based on the symmetry of actuator placement.

Design of portable grasping device

We developed an untethered device that can be used to operate soft robotic actuators in a laboratory or aquarium setting. The device uses a 12-V peristaltic pump (PM200F, Simply Pumps, PA) to open and close the actuators. The actuators and hub were fastened to one end of a carbon fiber rod, and the pump and batteries were housed in a waterproof box at the opposite side. An input tube connected to the pump drew water from the device's environment and facilitated rapid hydraulic actuation (actuators inflated in ~5 s) in a marine, laboratory, or aquarium setting.

Pilot study of jellyfish grasping

For *A. aurita* and *C. mosaicus*, a single jellyfish was placed in a transparent tank, and the hand-held robotic actuation device was used to carefully grasp and release the animal. The soft actuators were inserted into the tank (Fig. 7A), pressurized to roughly 5 psi as the actuators enclosed the jellyfish (Fig. 7, B and C), and then depressurized to allow the animal to swim away (movie S2). This procedure was repeated several times (n = 20 to 25 grasps) using multiple jellyfish (n = 2 to 4 per species). An aquarist was present to monitor the jellyfishes' behavior during the trials.

Statistical analysis

Analysis of variance (ANOVA) tests were used to analyze data sets, and error is reported as SD. P values below 0.05 were used to indicate statistical significance. Statistical comparisons of Bernoulli trials (success-failure experiments) during laboratory grasping were calculated using Agresti-Coull confidence intervals.

SUPPLEMENTARY MATERIALS

robotics.sciencemag.org/cgi/content/full/4/33/eaax5425/DC1

Text

Fig. S1. Schematic of grasp quality testing procedure.

Fig. S2. Contact pressure of soft actuators.

Fig. S3. Characterizing the shear strength of wet adhesion between soft actuators.

Fig. S4. Destructive grasp attempt of gelatinous acorn worm.

Fig. S5. Drag force versus soft gripper speed.

Fig. S6. Comparative failure pressure of fiber-reinforced and pure elastomer actuators.

Fig. S7. Caging grasps using soft robotic actuators.

Movie S1. Empirical evaluation of ultrasoft gripper performance using a custom-designed underwater testing platform.

Movie S2. Field testing of soft robotic gripper.

References (*60*–*67*)

REFERENCES AND NOTES

1. L. K. Grunenfelder, N. Suksangpanya, C. L. Salinas, G. W. Milliron, N. A. Yaraghi, S. A. Herrera, K. Evans-Lutterodt, S. R. Nutt, P. D. Zavattieri, D. Kisailus, Bio-inspired impact-resistant composites. *Acta Biomater.* **10**, 3997–4008 (2014).
2. L. Xiao, J. Li, S. Mieszkin, A. D. Fino, A. S. Clare, M. E. Callow, J. A. Callow, M. Grunze, A. Rosenhahn, P. A. Levkin, Slippery liquid-infused porous surfaces showing marine antibiofouling properties. *ACS Appl. Mater. Interfaces* **5**, 10074–10080 (2013).
3. A. K. Epstein, D. Hong, P. Kim, J. Aizenberg, Biofilm attachment reduction on bioinspired, dynamic, micro-wrinkling surfaces. *New J. Phys.* **15**, 095018 (2013).
4. M. Rangel, M. de Barcellos Falkenberg, An overview of the marine natural products in clinical trials and on the market. *J. Coast. Life Med.* **3**, 421–428 (2015).
5. P. Kiuru, M. Valeria D'Auria, C. D. Muller, P. Tammela, H. Vuorela, J. Yli-Kauhaluoma, Exploring marine resources for bioactive compounds. *Planta Med.* **80**, 1234–1246 (2014).
6. C. Laschi, M. Cianchetti, B. Mazzolai, L. Margheri, M. Follador, P. Dario, Soft robot arm inspired by the octopus. *Adv. Robot.* **26**, 709–727 (2012).
7. M. Cianchetti, M. Follador, B. Mazzolai, P. Dario, C. Laschi, Design and development of a soft robotic octopus arm exploiting embodied intelligence, in *2012 IEEE International Conference on Robotics and Automation (ICRA)* (IEEE, 2012), pp. 5271–5276.
8. F. Berlinger, M. Duduta, H. Gloria, D. Clarke, R. Nagpal, R. Wood, A modular dielectric elastomer actuator to drive miniature autonomous underwater vehicles, in *2018 IEEE International Conference on Robotics and Automation (ICRA)* (IEEE, 2018), pp. 3429–3435.
9. T. Li, G. Li, Y. Liang, T. Cheng, J. Dai, X. Yang, B. Liu, Z. Zeng, Z. Huang, Y. Luo, T. Xie, W. Yang, Fast-moving soft electronic fish. *Sci. Adv.* **3**, e1602045 (2017).
10. A. D. Marchese, C. D. Onal, D. Rus, Autonomous soft robotic fish capable of escape maneuvers using fluidic elastomer actuators. *Soft Robot.* **1**, 75–87 (2014).
11. J. Fras, Y. Noh, M. Macias, H. Wurdemann, K. Althoefer, Bio-inspired octopus robot based on novel soft fluidic actuator, in *2018 IEEE International Conference on Robotics and Automation (ICRA)* (IEEE, 2018), pp. 1583–1588.
12. T. K. Doyle, G. C. Hays, C. Harrod, J. D. R. Houghton, Ecological and societal benefits of jellyfish, in *Jellyfish Blooms*, K. A. Pitt, C. H. Lucas, Eds. (Springer, 2014), pp. 105–127.
13. W. M. Graham, S. Gelcich, K. L. Robinson, C. M. Duarte, L. Brotz, J. E. Purcell, L. P. Madin, H. Mianzan, K. R. Sutherland, S.-i. Uye, K. A. Pitt, C. H. Lucas, M. Bøgeberg, R. D. Brodeur, R. H. Condon, Linking human well-being and jellyfish: Ecosystem services, impacts, and societal responses. *Front. Ecol. Environ.* **12**, 515–523 (2014).
14. C. H. Lucas, D. O. B. Jones, C. J. Hollyhead, R. H. Condon, C. M. Duarte, W. M. Graham, K. L. Robinson, K. A. Pitt, M. Schildhauer, J. Regetz, Gelatinous zooplankton biomass in the global oceans: Geographic variation and environmental drivers. *Glob. Ecol. Biogeogr.* **23**, 701–714 (2014).
15. P. R. Pugh, Gelatinous zooplankton-the forgotten fauna. *Underwater Sci. Prog.* **14**, 67–78 (1989).
16. S. Piraino, F. Boero, B. Aeschbach, V. Schmid, Reversing the life cycle: Medusae transforming into polyps and cell transdifferentiation in *turritopsis nutricula* (cnidaria, hydrozoa). *Biol. Bull.* **190**, 302–312 (1996).

17. O. Shimomura, F. H. Johnson, Y. Saiga, Extraction, purification and properties of aequorin, a bioluminescent protein from the luminous hydromedusan, *Aequorea*. *J. Cell. Comp. Physiol.* **59**, 223–239 (1962).
18. V. Pieribone, D. F. Gruber, *Aglow in the Dark: The Revolutionary Science of Biofluorescence* (Harvard Univ. Press, 2005).
19. C. Gambini, B. Abou, A. Ponton, A. J. M. Cornelissen, Micro- and macrorheology of jellyfish extracellular matrix. *Biophys. J.* **102**, 1–9 (2012).
20. M. J. Abrams, T. Basinger, W. Yuan, C.-L. Guo, L. Goentoro, Self-repairing symmetry in jellyfish through mechanically driven reorganization. *Proc. Natl. Acad. Sci. U.S.A.* **112**, E3365–E3373 (2015).
21. D. Rudolf, D. Mould, An interactive fluid model of jellyfish for animation, in *International Conference on Computer Vision, Imaging and Computer Graphics* (Springer, 2009), pp. 59–72.
22. M. E. Demont, J. M. Gosline, Mechanics of jet propulsion in the hydromedusan jellyfish, *Polyorchis pexicillatus*: I. Mechanical properties of the locomotor structure. *J. Exp. Biol.* **134**, 313–332 (1988).
23. C. W. Dunn, P. R. Pugh, S. H. D. Haddock, *Marrus claudanielis*, a new species of deep-sea physonect siphonophore (siphonophora, physonectae). *Bull. Mar. Sci.* **76**, 699–714 (2005).
24. S. Sivčev, J. Coleman, E. Omerdić, G. Dooly, D. Toal, Underwater manipulators: A review. *Ocean Eng.* **163**, 431–450 (2018).
25. H. Stuart, S. Wang, O. Khatib, M. R. Cutkosky, The ocean one hands: An adaptive design for robust marine manipulation. *Int. J. Robot. Res.* **36**, 150–166 (2017).
26. K. C. Galloway, K. P. Becker, B. Phillips, J. Kirby, S. Licht, D. Tchernov, R. J. Wood, D. F. Gruber, Soft robotic grippers for biological sampling on deep reefs. *Soft Robot.* **3**, 23–33 (2016).
27. D. M. Vogt, K. P. Becker, B. T. Phillips, M. A. Graule, R. D. Rotjan, T. M. Shank, E. E. Cordes, R. J. Wood, D. F. Gruber, Shipboard design and fabrication of custom 3D-printed soft robotic manipulators for the investigation of delicate deep-sea organisms. *PLOS ONE* **13**, e0200386 (2018).
28. S. Licht, E. Collins, M. L. Mendes, C. Baxter, Stronger at depth: Jamming grippers as deep sea sampling tools. *Soft Robot.* **4**, 305–316 (2017).
29. C. Kelley, T. Kerby, P.-M. Sarradin, J. Sarrazin, D. J. Lindsay, Submersibles and remotely operated vehicles, in *Biological Sampling in the Deep Sea*, M. R. Clark, M. Consalvey, A. A. Rowden, Eds. (John Wiley & Sons, Ltd., 2016), pp. 285–305.
30. Z. E. Teoh, B. T. Phillips, K. P. Becker, G. Whittredge, J. C. Weaver, C. Hoberman, D. F. Gruber, R. J. Wood, Rotary-actuated folding polyhedrons for midwater investigation of delicate marine organisms. *Sci. Robot.* **3**, eaat5276 (2018).
31. J. B. C. Davies, D. M. Lane, G. C. Robinson, D. J. O'Brien, M. F. C. Pickett, M. Sfakiotakis, B. Deacon, Subsea applications of continuum robots, in *Proceedings of the 1998 International Symposium on Underwater Technology* (IEEE, 1998), pp. 363–369.
32. S. Licht, E. Collins, D. Ballat-Durand, M. Lopes-Mendes, Universal jamming grippers for deep-sea manipulation, in *OCEANS 2016 MTS/IEEE Monterey* (IEEE, 2016), pp. 1–5.
33. M. Zbinden, B. Shillito, N. Le Bris, C. de Villardi de Montlaur, E. Roussel, F. Guyot, F. Gaill, M.-A. Cambon-Bonavita, New insights on the metabolic diversity among the epibiotic microbial communitiy of the hydrothermal shrimp *Rimicaris exoculata*. *J. Exp. Mar. Biol. Ecol.* **359**, 131–140 (2008).
34. G. I. Matsumoto, K. A. Raskoff, D. J. Lindsay, *Tiburonia granrojo* n. sp., a mesopelagic scyphomedusa from the pacific ocean representing the type of a new subfamily (class scyphozoa: Order semaeostomeae: Family ulmaridae: Subfamily tiburoniinae subfam. nov.). *Mar. Biol.* **143**, 73–77 (2003).
35. N. R. Sinatra, T. Ranzani, J. J. Vlassak, K. K. Parker, R. J. Wood, Nanofiber-reinforced soft fluidic micro-actuators. *J. Micromech. Microeng.* **28**, 084002 (2018).
36. A. Sudsang, J. Ponce, A new approach to motion planning for disc-shaped robots manipulating a polygonal object in the plane, in *Proceedings of the 2000 IEEE International Conference on Robotics and Automation (ICRA'00)* (IEEE, 2000), vol. 2, pp. 1068–1075.
37. T. G. Nevell, D. P. Edwards, A. J. Davis, R. A. Pullin, The surface properties of silicone elastomers exposed to seawater. *Biofouling* **10**, 199–212 (1996).
38. K. P. Lee, T. C. Arnot, D. Mattia, A review of reverse osmosis membrane materials for desalination–Development to date and future potential. *J. Membr. Sci.* **370**, 1–22 (2011).
39. W. Xu, C. Ma, J. Ma, T. Gan, G. Zhang, Marine biofouling resistance of polyurethane with biodegradation and hydrolyzation. *ACS Appl. Mater. Interfaces* **6**, 4017–4024 (2014).
40. Z. Shen, J. Na, Z. Wang, A biomimetic underwater soft robot inspired by cephalopod mollusc. *IEEE Robot. Autom. Lett.* **2**, 2217–2223 (2017).
41. R. L. Baines, J. W. Booth, F. E. Fish, R. Kramer-Bottiglio, Toward a bio-inspired variable-stiffness morphing limb for amphibious robot locomotion, in *2019 2nd IEEE International Conference on Soft Robotics (RoboSoft)* (IEEE, 2019), pp. 704–710.
42. S. C. Shit, P. Shah, A review on silicone rubber. *Natl. Acad. Sci. Lett.* **36**, 355–365 (2013).
43. L. Bat, H. H. Satilmis, Z. Birinci-Ozdemir, F. Sahin, F. Ustun, Distribution and population dynamics of *Aurelia aurita* (cnidaria; scyphozoa) in the southern Black Sea. *North-Western J. Zool.* **5**, 225–241 (2009).
44. S. R. Boco, E. B. Metillo, R. D. Papa, Abundance, size and symbionts of *Catostylus sp. medusae* (scyphozoa, rhizostomeae) in Panguil Bay, Northern Mindanao, Philippines. *Phil. J. Syst. Biol.* **8**, 63–81 (2014).
45. D. M. Aukes, M. R. Cutkosky, Simulation-based tools for evaluating underactuated hand designs, in *2013 IEEE International Conference on Robotics and Automation (ICRA)* (IEEE, 2013), pp. 2067–2073.
46. C. Ferrari, J. Canny, Planning optimal grasps, in *1992 IEEE International Conference on Robotics and Automation (ICRA)* (IEEE, 1992), pp. 2290–2295.
47. X.-Y. Zhang, Y. Nakamura, K. Goda, K. Yoshimoto, Robustness of power grasp, in *Proceedings of the 1994 IEEE International Conference on Robotics and Automation* (IEEE, 1994), pp. 2828–2835.
48. A. Garm, M. O'Connor, L. Parkefelt, D.-E. Nilsson, Visually guided obstacle avoidance in the box jellyfish *Tripedalia cystophora* and *Chiropsella bronzie*. *J. Exp. Biol.* **210**, 3616–3623 (2007).
49. R. D. Nath, C. N. Bedbrook, M. J. Abrams, T. Basinger, J. S. Bois, D. A. Prober, P. W. Sternberg, V. Gradinaru, L. Goentoro, The jellyfish *Cassiopea* exhibits a sleep-like state. *Curr. Biol.* **27**, 2984–2990.e3 (2017).
50. P. J. Yang, M. Lemons, D. L. Hu, Rowing jellyfish contract to maintain neutral buoyancy. *Theor. Appl. Mech. Lett.* **8**, 147–152 (2018).
51. W. M. Hamner, P. P. Hamner, S. W. Strand, Sun-compass migration by *Aurelia aurita* (Scyphozoa): Population retention and reproduction in Saanich Inlet, British Columbia. *Mar. Biol.* **119**, 347–356 (1994).
52. D. Bhattacharya, S. Agrawal, M. Aranda, S. Baumgarten, M. Belcaid, J. L. Drake, D. Erwin, S. Foret, R. D. Gates, D. F. Gruber, B. Kamel, M. P. Lesser, O. Levy, Y. J. Liew, M. MacManes, T. Mass, M. Medina, S. Mehr, E. Meyer, D. C. Price, H. M. Putnam, H. Qiu, C. Shinzato, E. Shoguchi, A. J. Stokes, S. Tambutté, D. Tchernov, C. R. Voolstra, N. Wagner, C. W. Walker, A. P. M. Weber, V. Weis, E. Zelzion, D. Zoccola, P. G. Falkowski, Comparative genomics explains the evolutionary success of reef-forming corals. *eLife* **5**, e13288 (2016).
53. B. H. Robison, Deep pelagic biology. *J. Exp. Mar. Biol. Ecol.* **300**, 253–272 (2004).
54. M. S. Norouzzadeh, A. Nguyen, M. Kosmala, A. Swanson, M. S. Palmer, C. Packer, J. Clune, Automatically identifying, counting, and describing wild animals in camera-trap images with deep learning. *Proc. Natl. Acad. Sci. U.S.A.* **115**, E5716–E5725 (2018).
55. S. Mehr, A. Verdes, R. DeSalle, J. Sparks, V. Pieribone, D. F. Gruber, Transcriptome sequencing and annotation of the polychaete *Hermodice carunculata* (annelida, amphinomidae). *BMC Genomics* **16**, 445 (2015).
56. P. Polygerinos, Z. Wang, K. C. Galloway, R. J. Wood, C. J. Walsh, Soft robotic glove for combined assistance and at-home rehabilitation. *Robot. Autonom. Syst.* **73**, 135–143 (2015).
57. M. R. Badrossamay, H. A. McIlwee, J. A. Goss, K. K. Parker, Nanofiber assembly by rotary jet-spinning. *Nano Lett.* **10**, 2257–2261 (2010).
58. A. K. Capulli, M. Y. Emmert, F. S. Pasqualini, D. Kehl, E. Caliskan, J. U. Lind, S. P. Sheehy, S. J. Park, S. Ahn, B. Weber, J. A. Goss, S. P. Hoerstrup, K. K. Parker, JetValve: Rapid manufacturing of biohybrid scaffolds for biomimetic heart valve replacement. *Biomaterials* **133**, 229–241 (2017).
59. M. Quigley, K. Conley, B. Gerkey, J. Faust, T. Foote, J. Leibs, R. Wheeler, A. Y. Ng, ROS: An open-source Robot Operating System, in *ICRA Workshop on Open Source Software* (ICRA, 2009), vol. 3, pp. 5.
60. J. O. Dabiri, S. P. Colin, J. H. Costello, Morphological diversity of medusan lineages constrained by animal–fluid interactions. *J. Exp. Biol.* **210**, 1868–1873 (2007).
61. B. J. Gemmell, J. H. Costello, S. P. Colin, C. J. Stewart, J. O. Dabiri, D. Tafti, S. Priya, Passive energy recapture in jellyfish contributes to propulsive advantage over other metazoans. *Proc. Natl. Acad. Sci. U.S.A.* **110**, 17904–17909 (2013).
62. J. O. Dabiri, S. P. Colin, J. H. Costello, M. Gharib, Flow patterns generated by oblate medusan jellyfish: Field measurements and laboratory analyses. *J. Exp. Biol.* **208**, 1257–1265 (2005).
63. S. Alben, L. A. Miller, J. Peng, Efficient kinematics for jet-propelled swimming. *J. Fluid Mech.* **733**, 100–133 (2013).
64. J. H. Costello, S. P. Colin, J. O. Dabiri, Medusan morphospace: Phylogenetic constraints, biomechanical solutions, and ecological consequences. *Invertebr. Biol.* **127**, 265–290 (2008).
65. S. P. Colin, J. H. Costello, K. Katija, J. Seymour, K. Kiefer, Propulsion in cubomedusae: Mechanisms and utility. *PLOS ONE* **8**, e56393 (2013).
66. T. L. Daniel, Cost of locomotion: Unsteady medusan swimming. *J. Exp. Biol.* **119**, 149–164 (1985).
67. T. L. Daniel, Mechanics and energetics of medusan jet propulsion. *Can. J. Zool.* **61**, 1406–1420 (1983).

Acknowledgments: We would like to thank A. Varma and J. Jaacks for their photography and videography of the jellyfish field study. We greatly appreciate the New England Aquarium and the assistance of aquarists S. Spina and C. Doller in performing field testing using jellyfish. **Funding:** This work was performed in part at Harvard University's Center for Nanoscale

Systems (CNS), a member of the National Nanotechnology Coordinated Infrastructure Network (NNCI), which is supported by the National Science Foundation under NSF award no. 1541959. Research reported in this publication was supported by the Harvard University Materials Research Science and Engineering Center (award no. DMR-1420570), the National Science Foundation Graduate Research Fellowship (award no. DGE1745303), NSF IDBR (award no. DBI-1556164), the National Academies Keck Futures Initiative (award no. NAKFIDBS21), and the National Geographic Society (award no. PFA- RNG-2018-01). Any opinions, findings, and conclusions or recommendations expressed in this material are those of the authors and do not necessarily reflect the views of the National Science Foundation. **Author contributions:** N.R.S., C.B.T., D.M.V., D.F.G., and R.J.W. designed and performed all experiments. All authors contributed to the development of the research and the preparation of the manuscript.

Competing interests: The authors declare that they have no competing interests. **Data and materials availability:** All data needed to evaluate the conclusions in this paper are present in the paper or the Supplementary Materials.

Submitted 2 April 2019
Accepted 5 August 2019
Published 28 August 2019
10.1126/scirobotics.aax5425

Citation: N. R. Sinatra, C. B. Teeple, D. M. Vogt, K. K. Parker, D. F. Gruber, R. J. Wood, Ultragentle manipulation of delicate structures using a soft robotic gripper. *Sci. Robot.* **4**, eaax5425 (2019).

Ultragentle manipulation of delicate structures using a soft robotic gripper

Nina R. Sinatra, Clark B. Teeple, Daniel M. Vogt, Kevin Kit Parker, David F. Gruber and Robert J. Wood

Sci. Robotics **4**, eaax5425.
DOI: 10.1126/scirobotics.aax5425